Materials Chemistry Horizons RESEARCH

Nonlinear Optical Properties of Fluorescence Carbazole Derivative Using Continue Wave Blue Laser

Amir Hossein Ehsanian [1], Ehsan Koushki [1,*], Faezeh Ekhlasinia [2], Hamid Akherat Doost [1,3]

[1] Department of Physics, Hakim Sabzevari University, Sabzevar, 96179-76487, Iran
[2] Department of Chemistry, Hakim Sabzevari University, Sabzevar, 96179-76487, Iran
[3] Department of Physics, Central Tehran Branch, IAU, Tehran, Iran

Corresponding authors: ehsan.koushki@yahoo.com (E. Koushki)

Mater. Chem. Horizons, 2023, 2(1), 57-63 10.22128/mch.2022.616.1033 OPEN ACCESS

ABSTRACT

Nonlinear optical properties of synthesized carbazole based compound (9H-Carbazole-3,6-dicarboxaldehyde, 9-hexyl-) were investigated and measured using the Z-scan method with a continuous wave blue diode laser, in different laser intensities. Open aperture Z-scan curves have peak configuration which indicates saturation in absorption has occurred. In close aperture Z-scan measurements, a peak-valley configuration of Z-san curves was related to the thermal-lensing effect that was observed below 100mW incident power. At higher incident powers, because of high nonlinear optical phase change, diffraction rings patterns were observed. Besides the photoluminescence emission of Carbazole compounds under the emission of a blue laser beam, the high nonlinear optical properties of this compound indicate that it can be a potential candidate in optical devices.

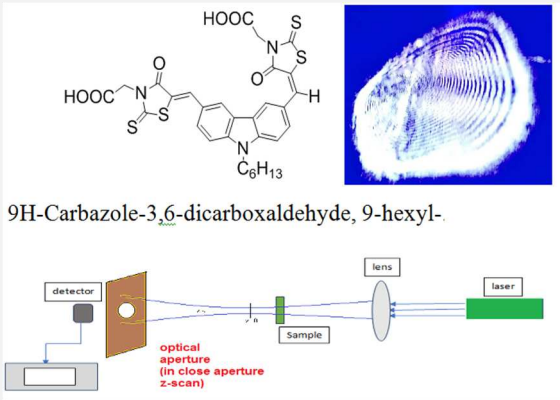

Keywords: Carbazole compounds, saturation absorption, photoluminescence, Z-scan technique, diffraction rings pattern

1. Introduction

In the last decades, using of optical materials has been extensively developed to meet the needs of optical technology and industry. One of the areas of interest in this regard is the field of non-linear optical materials, which have wide applications in light modulation. Various nanomaterials and organic materials are known as active nonlinear optical samples with high and fast responses in optical setups and instruments [1-3].

The optical properties of organic components are unique and considerable and they have attracted the attention of many researchers [4-6]. Molecules such as dyes and azo dyes compounds, as well as heterocyclic structures, have high chemical stability and fast optical response speed and exhibit optical and nonlinear optical behaviors [7,8]. Because their structure contains several π-electron conjugations, the nonlinear optical properties of organic materials are relatively high. Also, their synthesis is easy and accessible and they are recommended for optical devices [9]. Therefore, the kind of nonlinear optical process and its measurement method are very important.

One of the most important nonlinear optical responses of materials is the Kerr effect which is a third-order nonlinearity [10] that can be easily measured via the Z-scan method [11]. Today, many researchers know this technique that was first discovered by Sheikh Bahai and his colleagues [12]. This technique is still used and has many applications; it is simple and very sensitive in measuring the nonlinear optical properties of materials. To obtain nonlinear optical information of the material, it is enough to move the sample along the laser beam propagation. Changing the position of the sample relative to the focus of the laser gives us information in different places, which requires analysis. By measuring the laser transmission in the far field, the optical properties of the nonlinear material would be obtained. On the other hand, in the past decades, researchers have made many efforts to improve the

Received: October 02, 2022
Received in revised: November 11, 2022
Accepted: November 20, 2022

performance of the Z-scan method [13]. Now we see a variety of new techniques and theoretical predictions in the Z-scan technique that enhances its sensitivity [14].

One of the most important nonlinear absorption phenomena is saturation in absorption. Saturation in absorption saddens when the rate of photon absorption exceeds the rate of emissions. In a two electronic levels system, the higher level becomes saturated and no more photons would be absorbed. It leads to saturation in absorption and is an intensity-dependent phenomenon [15].

In this study, a Z-scan measurement of one of the synthesized carbazole derivative compounds (9H-carbazole-3,6-dicarboxaldehyde, 9-hexyl-) was performed and nonlinear absorption and refractive coefficients were obtained. Also, diffraction rings patterns due to nonlinear phase shifts were studied. Photoluminescence and high-order nonlinear optical properties of this material suggested it as an ideal case for optoelectronic, eye protectors, and mode-lucking devices [13,14].

2. Materials and methods

2.1. Synthesize of 9H-carbazole-3,6-dicarboxaldehyde, 9-hexyl

The synthesis route contains two steps that have been detailed below:

Synthesis of 9-hexyl-9H-carbazole (1a): 1-bromohexane (3.356 g, 0.02033 mol), carbazole (2.0 g, 0.01196mol) and sodium hydroxide (4.0g, 0.10046mol) were added in dimethylsulfoxide (DMSO) (30 mL), followed by heating at 110 ˚C for 12 h. After cooling to room temperature the resulting mixture was extracted with ethyl acetate (EA)/water and then dried with Na_2SO_4. The solvent was evaporated and the resulting crude solid was purified by column chromatography on neutral alumina by using hexane as a solvent to give a white solid with a yield of 90.4% (3.1 g). m.p. 64-65 ˚C, ^{1}H NMR ($CDCl_3$, ppm): δ= 8.18 (d, 2H, J= 7.6 Hz), 7.56-7.54 (m,2H), 7.52-7.46 (m, 2H), 7.31 (t, 2H,J= 7.2Hz), 4.33 (t, 2H,J= 7.2Hz), 1.96-1.89 (m, 2H), 1.54-1.37 (m, 6H), 0.96 (d, J= 6.8 Hz,3H,) (see **Scheme 1**).

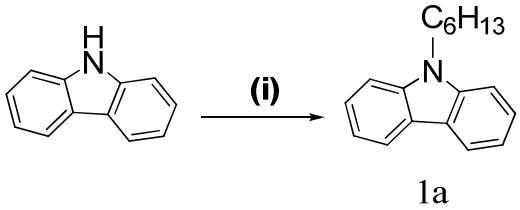

Scheme1. 9-hexyl-9H-carbazole

Synthesis of 9-hexyl-9H-carbazole-3,6-dicarbaldehyde: Phosphorus oxychloride (2.8 ml, 30mmol) was added dropwise to DMF (3.0 mL, 40 mmol) at 0 ˚C, and the mixture was stirred for 1 h at this temperature. Compound1a (5.05 g, 20 mmol) was added and the reaction mixture was stirred at 100 ˚C for 6h. Then, the mixture was cooled to room temperature, poured into ice water, and carefully neutralized with sodium hydroxide. The solution was extracted with dichloromethane (3 ×50 mL). The organic phase was washed with water (2 × 50 mL) and dried over anhydrous sodium sulfate. After filtration, the solvent was removed. The crude product was purified by silica gel column chromatography (ethyl acetate/petroleum ether, 1/10, v/v). The product was obtained as a white powder. Yield: 4 g (65%). H-NMR is described by (300 MHz, DMSO): δ 8.62(s, 2H), 8.08(s, 2H), 7.89(d, J = 8.7 Hz, 2H), 7.81(d, J = 8.7 Hz, 2H), 4.77(s, 4H), 4.48(t, J = 7.2 Hz, 2H), 1.80–0.78(m, 11H).). H-NMR,(300 MHz, $CDCl_3$): δ 10.14(s, 2H), 8.68(s, 2H), 8.10(d, J =8.7 Hz, 2H), 7.56(d, J = 8.7 Hz, 2H), 4.40(t, J = 7.2 Hz, 2H), 1.94–0.84 (m, 11H) (**Scheme 2**).

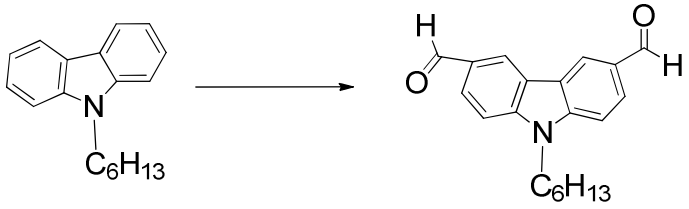

Scheme 2. 9-hexyl-9H-carbazole-3,6-dicarbaldehyde

In a dried 100 ml, round bottom flask, 9-hexyl-9H-carbazole-3,6-dicarbaldehyde (0.15 g, 0.48 mmol), rhodanine acetic acid (0.12 g, 0.63 mmol) ammonium acetate (0.054 g, 0.63mmol) were dissolved in acetic acid (30 ml). After heating the solution at 110 ˚C for 10 h, the solvent was evaporated to obtain an orange solid (**Scheme 3**).

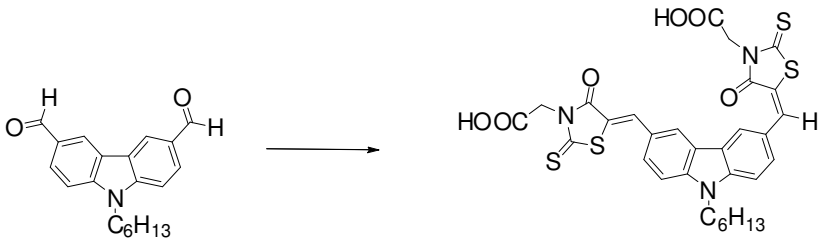

Scheme 3. 9H-Carbazole-3,6-dicarboxaldehyde, 9-hexyl-

2.2. Z-scan theory

In **Figure.1**, the experimental setup of the close aperture Z-scan technique is shown. This setup which is used for obtaining nonlinear refractive index (n_2), contains an optical aperture that determines the beam profile and it leads to the setup sensitivity to changes in refractive index (n) which depends on intensity (I) [16]:

$$n = n_0 + n_2 I \quad (1)$$

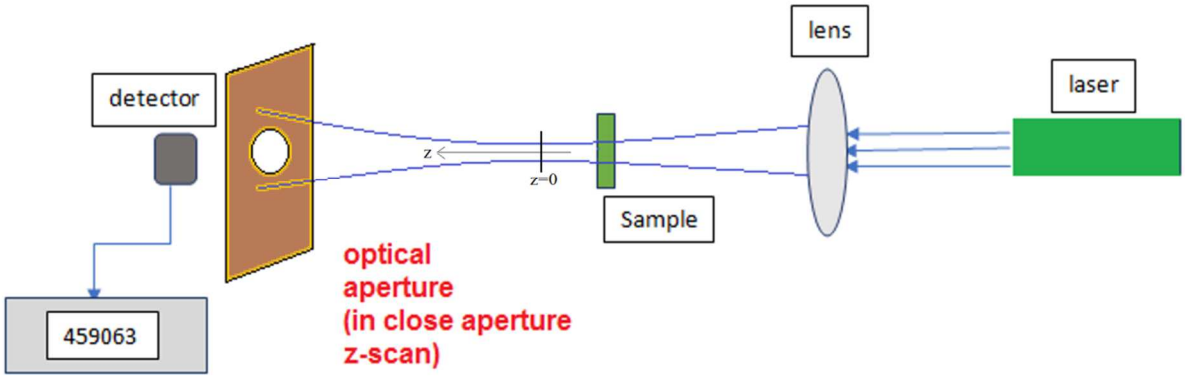

Figure 1. Schematic of close aperture Z-scan setup.

Also, the nonlinear absorption coefficient is measured using open aperture Z-scan measurement when the aperture is removed. The absorption coefficient (α) depends on the laser intensity and changes accordingly:

$$\alpha = \alpha_0 + \beta I \quad (2)$$

Where β is the nonlinear absorption coefficient. In the closed aperture Z-scan measurement, the sample examines different positions before and after the focal point while moving parallel to the z direction. According to the position of the sample (z) and the radius of the light beam, the transmitted power changes, and by drawing the curve of normalized transmittance against z, a close aperture Z-scan curve would be obtained which we get n_2 by fitting the experimental and theoretical curve. We get the far field at the plane of the aperture (Z+D) [16,17]:

$$E(r, z+D) = E_{in}(r=0, z)e^{-\alpha L/2}\sum_{m=0}^{\infty}\frac{[-i\Delta\varphi(z, r=0)]^m}{m!}\frac{w_{m0}}{w_m}\exp(-\frac{r^2}{w_m^2} - \frac{ikr^2}{2R_m} + i\theta_m) \quad (3)$$

D is the distance between the aperture and the sample and the electric field of the incident beam on the sample plane, other parameters are: k the wavenumber, L is the sample thickness, r is the radial coordinate, and the phase change that the beam exhibits in its center. The phase change is given by:

$$\Delta\varphi(z, r) = \frac{kn_2 I_0 L_{eff}}{1+(\frac{z}{z_0})^2}\exp(-2r^2/w^2(z)) \quad (4)$$

and also L_{eff}= (1-e$^{\alpha L}$)/α. Also, z_0 is the effective length of the sample and z_0 is Rayleigh length, and I_0 is the intensity at the center of the beam waist. Now by defining g= 1+D/R(z), we will achieve new relations:

$$w_{m0}^2 = \frac{w^2(z)}{2m+1}, \quad d_m = \frac{kw_{m0}^2}{2}, \quad w_m^2 = w_{m0}^2[g^2 + \frac{D^2}{d_m^2}], \quad R_m = D[1 - \frac{g}{g^2 + D^2/d_m^2}]^{-1},$$
$$\theta_m = \tan^{-1}[\frac{D/d_m}{g}] \tag{5}$$

We can get the transmitted power from the following relation:

$$P(z) = \int_0^{r_a} I(r,z) 2\pi r dr \tag{6}$$

In closed aperture Z-scan measurement, we can write the normalized transmittance at any point as follows:

$$T(z) = \frac{\int_0^{\infty} P(z, \Delta\varphi_0(t)) dt}{\int_0^{\infty} P(z, \Delta\varphi_0 = 0) dt} \tag{7}$$

.

by comparing experimental data with the theoretical curve, n_2 would be obtained. To perform open aperture Z-scan measurement, we must remove the aperture and expose the sample to the light laser. Here we measure the transmitted power at any point of z, which we refer to below [9,10]:

$$P(z) = P_0 e^{-\alpha L} \frac{Ln(1+q_0(z))}{q_0(z)} \tag{8}$$

where $q_0(z) = \frac{\beta I_0 L_{eff}}{(1+(z/z_0)^2)}$. Using Eq.8 and curve fitting, we can obtain β.

2.3. Z-scan experiment

We consider a Z-scan setup consisting of a laser, a lens, and a detector, as shown in **Figure 1**. The laser beam has a circular symmetric field and propagates in the Z direction. The lens is placed perpendicular to the z direction. The laser light beam has been focused by the convergent lens with a focal point of 8cm and the quart cell containing the synthesized material is placed near the focus and moves along the z direction. The thickness of the cell is 1 mm.

Our experimental setup was containing a continuous wave (CW) blue diode laser with a wavelength of 450 nm (CNlaser/MSL-S-532-S) according to the arrangement of the Z-scan setup. Optical powers transmitted through the samples were measured using a semiconductor photo-detector (Ashabeam/ PMB-101/IRAN) to obtain z-scan curves.

We performed the open and closed diaphragm measurements and obtained the corresponding curves. The output power of our laser was 500mW. We used a lens with a focal length of 8 cm to focus the laser light. To measure the waist, we proceeded according to the edge scanning technique, and w_0 = 35 μm obtained the beam waist at the focal point [7,16]. We prepared solutions of the mentioned compound with a concentration of 5 mM and poured them into the quartz cell. The circular aperture with a radius of r_a = 0.2 mm was used for the close aperture setup.

3. Results and discussion

According to **Figures 2** and **3**, we have the peak-valley distortion for the closed aperture experiment that indicates n_2 is a negative value for powers of 50 and 100 mW. In **Table 1**, the values of the nonlinear refractive index are reported, which are negative. These values are more related to the thermal lensing effect rather than the electronic energy levels [18,19]. It should be noted that in low laser intensities, the origin of nonlinear optical properties with a very small percentage of contribution is related to electronic energy levels [7,12,16]. In the thermal lensing effect, when the laser light hits the desired material at the point of irradiation, heat is generated and the temperature rises, so at this point, we will have local expansion and the material will be diluted. As a result of this action, the refractive

index will decrease. Increasing the power from 50 to 100 mW, n_2 was increased which is attributed to more thermal expansion and optical phase shift.

By increasing the laser intensity, a diffraction ring pattern was observed that indicates high-order nonlinear optical phase shift [20]. The high value of induced nonlinear phase shift diffracts the laser beam in the form of ring patterns [21]. These rings make measuring close aperture data difficult, because of the unstable power transmitted from the finite aperture and high fluctuations in the curve.

Table 1. The values obtained from the Z-scan measurements.

	P=50 mW	P=100 mW	P=300 mW	P=500 mW
I_0 (W/cm^2)	2600	5200	15600	26000
β(cm/W)	-1.51×10^{-4}	-1.69×10^{-4}	-2.32×10^{-4}	-2.89×10^{-4}
n_2(cm^2/W)	-1.51×10^{-4}	-1.90×10^{-7}	Diffraction rings	Diffraction rings
Δn	-4.41×10^{-4}	-9.87×10^{-4}	Diffraction rings	Diffraction rings
$\Delta\varphi_0$	6.13	13.71	Diffraction rings	Diffraction rings

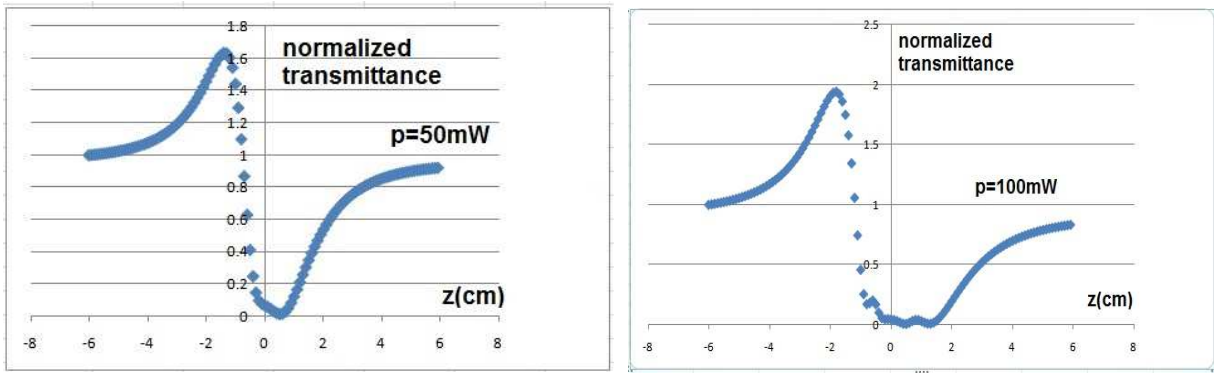

Figure 2. Diagrams of close aperture curves.

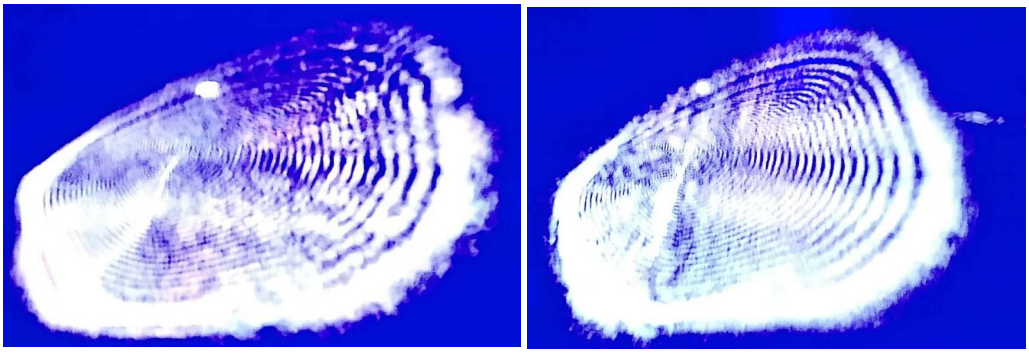

Figure 3. Image of diffraction rings at 300 mW intensities.

Open aperture curves have been obtained and plotted in **Figure 4**. As shown, the peak configuration indicates that saturation in absorption has occurred [22]. Using Eq.8, the values of β were obtained and reported in **Table 1** which indicates a direct relation between β and the laser intensity. It shows that the nonlinear absorption is not a constant coefficient. Materials with high saturation in absorption are mainly used in mode lucking devices and this material can be a good candidate for this purpose [23].

Finally, the photoluminescence of the solution was observed using a diode ultraviolet light source (λ=385nm). As shown in **Figure 5**, the solution of this compound can turn the violet light to green with high efficiency.

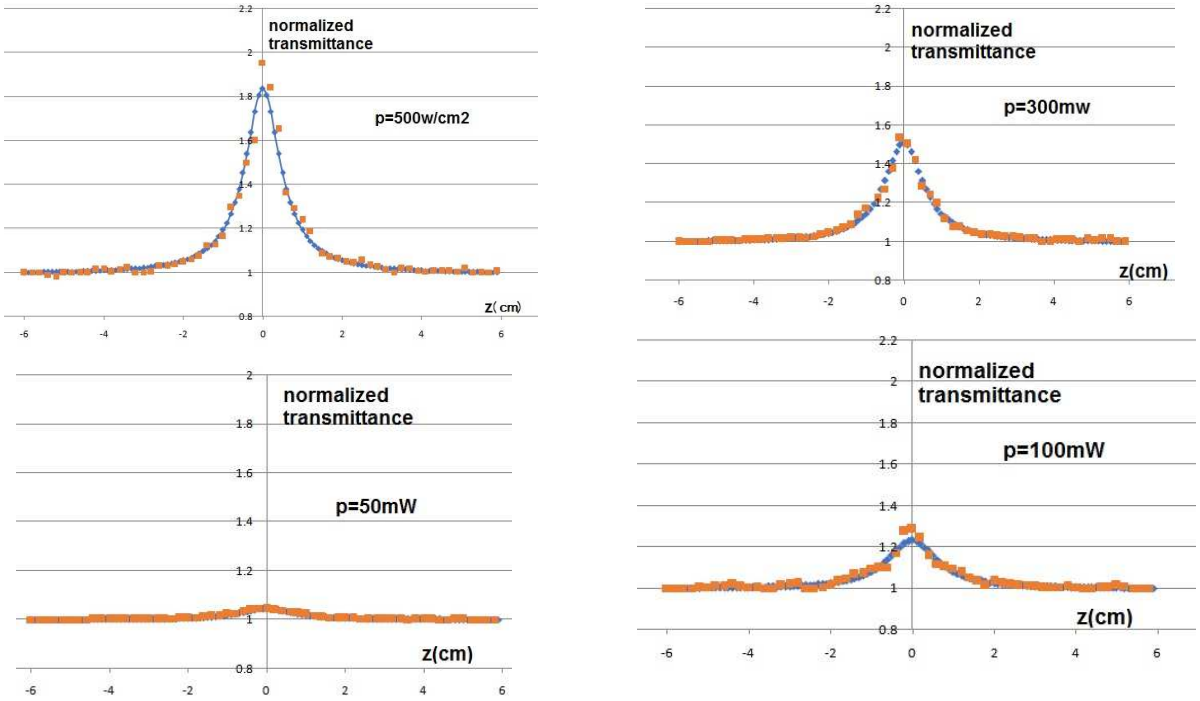

Figure 4. Open valve diagram with 50mW intensity.

Figure 5. Greenish fluorescence light produced by the material in the violet light radiation

4. Conclusions

In summary, nonlinear refractive and absorption indexes of a derivative of carbazole component were studied using the well-known Z-scan experiment with a 500 mW blue CW laser. Besides the high photoluminescence property of the material, the high-order nonlinear Kerr effect of the compound was studied. It was found that the open aperture curve has a peak form that indicates a negative value for the nonlinear absorption coefficient and indicates saturation in absorption occurred. In close aperture Z-scan measurements, a peak-valley configuration of curves can be related to the thermal-lensing effect that was observed below 100 mW incident power. At higher incident powers, because of high nonlinear optical phase change, diffraction rings patterns were observed. In conclusion, this material is recommended for optical devices and applications such as optical modulators and mode-locking apertures.

Authors' contributions

All authors contributed to drafting, and revising of the paper and agreed to be responsible for all the aspects of this work.

Declaration of competing interest

The authors declare no competing interest.

Funding

This paper received no external funding.

Data availability

Data will be made available on request.

References

[1] S. D. Durbin, S. M. Arakelian, and Y. R. Shen, Laser-induced diffraction rings from a nematic-liquid-crystal film, Opt. Lett. 6 (1981) 411-413.
[2] M. Safa, Y. Rajabi, M. Ardyanian, Influence of preparation method on the structural, linear, and nonlinear optical properties of TiN nanoparticles, J. Mater. Sci.: Mater. Electron. 32 (2021) 19455–19477.
[3] A. Alizadeh, Y. Rajabi, M.M. Bagheri–Mohagheghi, Effect of crystallinity on the nonlinear optical properties of indium–tin oxide thin films, Opt. Mater.131 (2022) 112589.
[4] A. Alizadeh, S. Rostamnia, N. Zohreh, R. Hosseinpour, A simple and effective approach to the synthesis of rhodanine derivatives via three-component reactions in water, Tetrahedron Lett. 50 (2009) 1533-1535.
[5] B. Li, L. Gao, H. Yi, L. Yang, Y. Song, Liming Zhou, And S. Fang, Synthesis and nonlinear optical properties of 4-phenylethylene, derivatives based on a large π conjugated structure, Opt. Mater. Express. 12 (2022) 1352.
[6] E. Koushki, B. Maleki, Induced photoacoustic gratings due to Raman scattering in organic components, Dyes Pigm.164 (2019) 82–86.
[7] M.H. Majles Ara, S.H. Mousavi, E. Koushki, S. Salmani, A .Gharibi, A. Ghanadzadeh, Nonlinear optical responses of Sudan IV doped liquid crystal by z-scan and moiré deflectometry techniques, J. Mol. Liq. 142 (2008) 29-31.
[8] R. Fathima, A. Mujeeb, Plasmon enhanced linear and nonlinear optical properties of natural curcumin dye with silver nanoparticles, Dyes Pigm. 189 (2021) 109256.
[9] T. R. Kumar, R. J. Vijay, R. Jeyasekaran, S. Selvakumar, M. A. Arockiaraj, and P. Sagayaraj, Growth, linear and nonlinear optical and, laser damage threshold studies of organometallic crystal of $MnHg(SCN)_4$, Opt. Mater. 33 (2011) 1654–1660.
[10] X. Lu, J. Y. Lee, S. Rogers, and Q. Lin, Optical Kerr nonlinearity in a high-Q silicon carbide microresonator, Opt. Express, 22 (2014) 30826-30832.
[11] G. Tsigaridas, M. Fakis, I. Polyzos, P. Persephonis, V. Giannetas, Z-scan analysis for high order nonlinearities through Gaussian decomposition, Opt. Comm. 225 (2003) 253-268.
[12] M. Sheik-Bahae, A.A. Said, T-H. Wei, D. J. Hagan, E. W. Van Stryland, Sensitive measurement of optical nonlinearities using a single beam, IEEE J. Quantum Electron. 26 (1990) 760-769.
[13] M.H. Majles Ara, E. Koushki, Data analysis of z-scan experiment using Fresnel–Kirchoff integral method in colloidal TiO_2 nanoparticles, Appl. Phys. B, 107 (2012) 429-434.
[14] C.B. Yao, K.X. Zhang, X. Wen, Focus introduction: Z-scan technique, Optik.140 (2017) 680-682.
[15] E. Koushki, M.H. Majles Ara, H. Akherat Doost, Z-scan technique for saturable absorption using diffraction method in γ-alumina nanoparticles, Appl. Phys. B 115 (2014) 279-284.
[16] B. Maleki, E. Koushki, H. Alinezhad, M. Tajbakhsh, A. H. Ehsanian, Z. Arab, S. Peiman, F. Ghasempour Nesheli, Low power Z-scan study and photoacoustic behavior of synthesized conjugated organic compounds based on carbazole derivatives, Opt. Mater. 128 (2022) 112377.
[17] B. Maleki, E. Esmaeilnezhad, H.J. Choi, E. Koushki, H. A. Rahnamaye Aliabad, M. Esmaeili, Glutathione-capped core-shell structured magnetite nanoparticles: Fabrication and their nonlinear optical characteristics, Curr. Appl. Phys. 20 (2020) 822-827.
[18] L. Palfalvi, J. Hebling, Z-scan study of the thermo-optical effect, Appl. Phys. B 78 (2004) 775–780.
[19] E. Koushki, A. Farzaneh, Time dependence of thermo-optical effect for thin samples containing light-absorptive material, Opt. Commun. 285 (2012) 1390–1393.
[20] E. Koushki, A. Farzaneh, S.H. Mousavi, Closed aperture z-scan technique using the Fresnel–Kirchhoff diffraction theory for materials with high nonlinear refractions, Appl. Phys. B, 99 (2010) 565-570.
[21] J. Li, Z. Zhang, J. Yi, L. Miao, J. Huang, J. Zhang, Y. He, B. Huang, C. Zhao, Yanhong Zou and S. Wen. Broadband spatial self-phase modulation and ultrafast response of MXene $Ti_3C_2T_x$ (T=O, OH or F). Nanophotonics. 9 (2020) 2415-2424.
[22] E. Koushki, M.H. Majles Ara, H. Akherat Doost, Z-scan technique for saturable absorption using diffraction method in γ-alumina nanoparticles, Appl. Phys. B, 115 (2014) 279-284.
[23] M. Suzuki, O. Boyraz, H. Asghari&B. Jalali, Spectral dynamics on saturable absorber in mode-locking with time stretch spectroscopy, Sci. Rep.10 (2020) 14460.